RSC Advances

PAPER

View Article Online
View Journal | View Issue

Cite this: *RSC Adv.*, 2017, 7, 22845

Effect of alkylthiophene spacers and fluorine on the optoelectronic properties of 5,10-bis(dialkylthien-2-yl)dithieno[2,3-*d*:2′,3′-*d*′]benzo[1,2-*b*:4,5-*b*′]dithiophene-*alt*-benzothiadiazole derivative copolymers†

Pengzhi Guo,[a] Jingbiao Sun,[a] Shuo Sun,[b] Jianfeng Li,[a] Junfeng Tong,[a] Chuang Zhao,[a] Liangjian Zhu,[a] Peng Zhang,[a] Chunyan Yang[a] and Yangjun Xia *[ac]

Received 29th December 2016
Accepted 14th April 2017

DOI: 10.1039/c6ra28836g

rsc.li/rsc-advances

Alternating conjugated copolymers based on 5,10-bis(dialkylthien-2-yl)dithieno[2,3-*d*:2′,3′-*d*′]benzo[1,2-*b*:4,5-*b*′]dithiophene (DTBDT) and 2,1,3-benzothiadiazole (BT) or 5,6-difluoro-2,1,3-benzothiadiazole (FBT) with alkylthiopene spacers were synthesized, and the effect of insertion of alkylthiophene spacers and fluorine atoms on the characteristics of the copolymers, such as the energy levels, intrachain π–π interaction, dielectric constants, photovoltaic properties, *etc.*, were systematically investigated. It has been found that: (i) the introduction of alkylthiophene spacers not only led to an increase in the intrachain interaction of the copolymers, but also resulted in an increase in the highest occupied molecular orbital (HOMO) levels and the lowest unoccupied molecular orbital (LUMO) levels, and (ii) the inclusion of fluorine atoms resulted in a decrease in both HOMO and LUMO energy levels with enhancement of the planarity and hole mobility. However, the inclusion of fluorine atoms had little effect on the LUMO levels relative to the decrease in the HOMO levels, and almost did not affect the dielectric constant of the copolymers. Use of the materials in polymeric photovoltaic cells led to high performance photovoltaic cells (PVCs) with power conversion efficiencies of 6.04–7.12%. The results demonstrated that the optoelectronic and aggregation properties of the 5,10-bis(alkylthien-2-yl)dithieno-[2,3-*d*:2′,3′-*d*′]benzo[1,2-*b*:4,5-*b*′]dithiophene-*alt*-benzothiadiazole derivative copolymers can be effectively regulated by the introduction of alkylthiophene spacers and/or fluorine atoms into the backbone.

1. Introduction

As a notable aromatic analogue of benzo[1,2-*b*:4,5-*b*′]dithiophene (BDT) – a most promising electron donor building block for high performance polymeric photovoltaic cells (PVCs) – dithieno[2,3-*d*:2′,3′-*d*′]benzo[1,2-*b*:4,5-*b*′]dithiophene (DTBDT) not only shows a similar highest occupied molecular orbital (HOMO) energy level to BDT, but also has a larger coplanar core and extended conjugation length.[1,2] It was believed to provide advantageous properties for DTBDT-based conjugated polymers (CPs) such as enhanced charge-carrier mobility, decreased band gaps and facilitated exciton separation into free charge carriers in contrast to BDT-based CPs.[2] The DTBDT-based CPs have attracted much attention in the development of novel high performance CPs for PVCs, since Hou *et al.* first reported a low band gap conjugated polymer (PDTT) with 5,10-di(2-hexyldecyloxy)-DTBDT as electron donor building blocks in 2012.[1b] After that, many promising CPs with DTBDT derivatives as electron donor moieties and the thieno[3,4-*b*]-thiophene (TT),[1b,2] 1,4-diketopyrrolo[3,4-*c*]pyrrole (DPP),[3] thieno[3,4-*c*]-pyrrole-4,6-dione (TPD),[4] dithieno[3,2-*b*:2′,3′-*d*]phosphole oxide (DPT),[5] naphtho[1,2-*c*:5,6-*c*′]bis[1,2,5]-thiadiazole (NT),[6] 2,1,3-benzothiadiazole (BT),[1d,7] isoindigo (ID),[8] 1,3-bis(thien-2-yl)-5,7-bis(2-ethylhexyl)-4*H*,8*H*-benzo[1,2-*c*:4,5-*c*′]dithiophene-4,8-dione[9] *etc.* derivatives as electron acceptor moieties have been presented, and the power conversions efficiencies (PCEs) of 4.0–9.7% have been demonstrated in the PVCs from the copolymers. Among them, the alternating co-polymer derived from 5,10-bis(4,5-didecylthien-2-yl)dithieno[2,3-*d*:2′,3′-*d*′]benzo-[1,2-*b*:4,5-*b*′]dithiophene (DTBDT-T) as electron donor moieties and 5,6-difluoro-2,1,3-benzothiadiazole (FBT) as electron acceptor moieties has been demonstrated to be a promising candidates for high performance PVCs, as it not only exhibited

[a]*Key Lab of Optoelectronic Technology and Intelligent Control of Education Ministry, Lanzhou Jiaotong University, Lanzhou, Gansu Province, 730070, China. E-mail: yjxia73@126.com*

[b]*National Laboratory for Infrared Physics, Shanghai Institute of Technical Physics, Chinese Academy of Sciences, Shanghai 200083, China*

[c]*Centre for Polymers and Organic Solids, University of California, Santa Barbara, CA 93106-9510, USA*

† Electronic supplementary information (ESI) available. See DOI: 10.1039/c6ra28836g

attracting photovoltaic properties, but also presented high photo-stability.[7]

In general, ideal polymeric photovoltaic electron donor CPs are required to have a broad and strong absorption, high carrier mobility and suitable energy levels, as well as appropriate miscibility with the fullerenes.[10] In spite of the fact that the incorporating electron-donor (D) moiety and electron-acceptor (A) moiety in the polymer backbone has been demonstrated to be the most efficient and common approach to modulate and optimize the optoelectronic and aggregation properties of the CPs for PVCs to date, the approach like of insertion of π-spacers between the D and A units have also been well proven to be other promising approach to alter the optoelectronic properties of polymers and miscibility of the polymers with the fullerene derivatives significantly.[11] For instance, Wang and co-workers reported a series of polymers containing BDT and isoindigo units by inserting bithiophene spacer to modulate the optoelectronic and aggregation properties of the co-polymers, and remarkable enhancement of PCEs from 2.8% to 7.3% for PVCs from the copolymers with bithiophene as π-spacers, have been achieved.[12a] Wei *et al.* demonstrated that the insertion of thiophene spacers can impart crystallinity and enhance the PCEs of the PVCs from benzotrithiophene-based CPs.[12b]

Herein, we modulated the optoelectronic properties of the copolymers with DTBDT-T as electron donor moieties and BT and FBT as electron acceptor moieties *via* the insertion of alkylthiophene as π-spacers. The influence of the insertion of the alkylthiophene spacers and fluorine atoms into the polymer backbone on the light absorption characteristics, energy levels, hole transporting properties, intrachain interaction in diluted solution and solid states, dielectric constant and photovoltaic properties *etc.* of the copolymers were systematically investigated. The results demonstrated that the optoelectronic and aggregation properties of the 5,10-bis(alkylthien-2-yl)dithieno-[2,3-*d*:2′,3′-*d*′]benzo[1,2-*b*:4,5-*b*′]-dithiophene-*alt*-benzothiadiazole derivatives copolymers can be effectively regulated by the introduction of alkylthiophene spacers and/or fluorine atoms into the polymer backbone.

2. Results and discussion

2.1. Synthesis and characterization of the copolymers

The general synthetic routes toward copolymers are outlined in Scheme 1. 2,7-Bis(trimethylstannyl)-5,10-di(4,5-didecyl-thien-2-yl)-DTBDT (DTBDT-TSn),[3a] 4,7-bis(5-bromo-4-octylthien-2-yl)-2,1,3-benzothiadiazole ($DTBTBr_2$) and 4,7-bis(5-bromo-4-dodecylthien-2-yl)-2,1,3-benzothiadiazole ($DTBTC12Br_2$),[13] 4,7-bis(5-bromo-4-octylthien-2-yl)-5,6-di-fluoro-2,1,3-benzothiadiazole ($DTFBTBr_2$) and 4,7-bis(5-bromo-4-dodecylthien-2-yl)-5,6-difluoro-2,1,3-benzothiadiazole ($DTFBTC12Br_2$)[14] were synthesized as the procedure reported in the corresponding references. The structures of the monomers were confirmed by ^{1}H NMR and elemental analyses before use. The copolymers were synthesized from the polymerization of DTBDT-TSn and BT derivatives like of $DTBTBr_2$ and $DTFBTBr_2$ *via* the palladium-catalysed Stille coupling reaction under mono-microwave heating condition,[15] followed with the end-capped reaction with 2-(tributylstannyl)thiophene and 2-bromothiophene to remove the bromo and trimethylstannyl end groups.[16] The number-average molecular weights of the copolymers determined by gel permeation chromatograph (GPC) in tetrahydrofuran (THF) with polystyrene standards, are about 2.61 × 10^4 and 3.74 × 10^4 g mol^{-1} with corresponding polydispersity index (PDI = M_w/M_n) of 2.46 and 3.17 for PDTBDT-DTBT and PDTBD-DTFBT, respectively (Table 1). The decomposed temperature (T_d, 5% weight-loss) of the copolymers are ranging from 410.3 to 423.6 °C (see ESI, Fig. S1†). It demonstrated that the copolymers exhibited excellent thermal-stability.

2.2. Optical properties of the copolymers

Firstly, we employed UV-vis absorption spectroscopy to characterize the absorption properties of the copolymers in dilute solution and solid state. As shown in Fig. 1a and b, the absorption spectra of PDTBDT-DTBT exhibited a 0–0 absorption peak at 680 nm and two well-resolved shoulder peaks as 0–1 and 0–2 at 630 nm and 474 nm with the optical band gap (E_g) of 1.63 eV in dilute solution. Meanwhile, the absorption spectra of PDTBDT-DTFBT exhibited a 0–0 absorption peak at 662 nm and two well-resolved shoulder peaks as 0–1 and 0–2 at 612 nm and 463 nm with the E_g of 1.72 eV. It could be found that the two

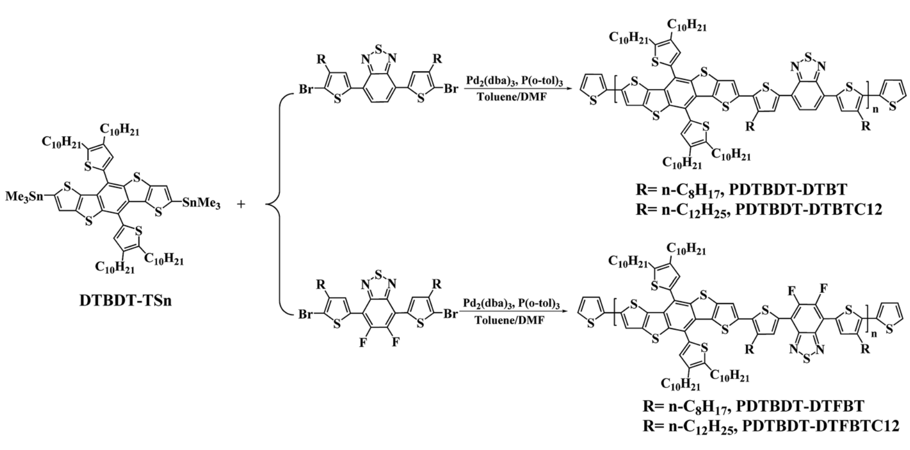

Scheme 1 Synthesis route of the copolymers.

Table 1 Molecular and optoelectronic parameters of the PDTBDT-DTBDT and PDTBDT-DTFBT

Copolymer	M_n (g mol^{-1} ($\times 10^3$))	M_w (g mol^{-1} ($\times 10^3$))	PDI	E_g^{opt} in film (eV)	E_{ox} (V)	HOMO (eV)	LUMO^a (eV)	Hole mobility (cm^2 V^{-1} s^{-1})	Relative dielectric constant	$V_{oc}^{Cal b}$ (V)	$V_{oc}^{Dev c}$ (V)	T_d (°C)
PDTBDT-DTBT	26.1	64.2	2.46	1.61	0.48	−5.19	−3.57	1.28×10^{-4}	2.86	0.67	0.63–0.66	410.3
PDTBDT-DTFBT	37.4	118.3	3.17	1.70	0.57	−5.28	−3.57	2.17×10^{-4}	2.85	0.76	0.72–0.73	423.6

^{a} Calculated from the HOMO energy levels and optical band gap of the copolymers in film by the empirical equation of $E_{LUMO} = -(|HOMO| - E_g)$ (eV). ^{b} calculated from the difference between LUMO the $PC_{71}BM$ and HOMO by empirical equation of $V_{oc} = (|HOMO^{Donor}| - |HOMO^{Donor}| - 0.3)/e$ (V). ^{c} Open circuit voltage of the PVCs from the copolymers and $PC_{71}BM$ blend films.

copolymers presented similar absorption characteristics in dilute solution and solid state except that the on-set band gap wavelengths were slightly red-shifted about 8–9 nm from solution to solid thin films. The main absorption peaks at 630 and 612 nm should be attributed to the intramolecular charge transfer (ICT) between electron-rich unit DTBDT and electron-deficient moieties BT and/or FBT along the conjugated backbones,[17] while the absorption peaks in high-energy region could arise from the localized π–π* transitions. And the shoulder peaks at 680 and 662 nm should be attributed to intermolecular π–π* transitions owing to the aggregation for the polymer chains.[18] As compared with the absorption spectra of the corresponding copolymers without alkylthiophene spacers, which were accordingly derived from DTBDT-T and BT and FBT, and named PDTBDT-BT and PDTBDT-FBT (see ESI, Fig. S2†), the band gaps of the PDTBDT-DTBT and PDTBDT-DTFBT exhibited narrower band gaps in contrast to those for the corresponding copolymers without alkylthiophene spacers (PDTBDT-BT and PDTBDT-FBT). In parallel, it also could be found that the on-set band gap wavelengths and main absorption peaks at around 658 nm for PDTBDT-BT and 646 nm for characteristics of the PDTBDT-DTBT and PDTBDT-FBT were clearly red-shifted, while the absorption PDTBDT-DTFBT were almost did not change from solution to solid state, which suggested that the PDTBDT-DTBT and PDTBDT-DTFBT have established strong interchain π–π* interaction even in dilute solution.[11e,14b]

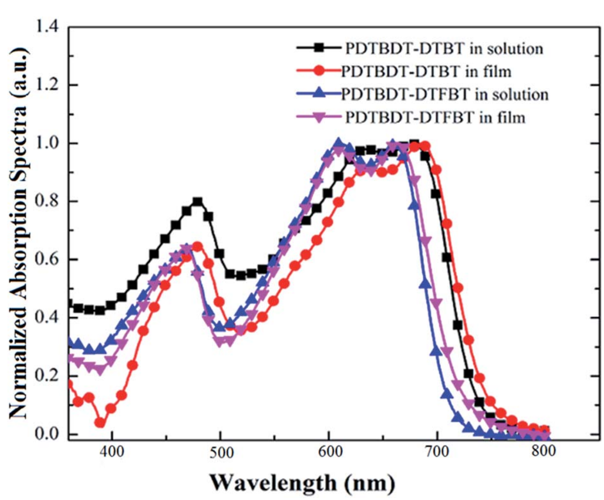

Fig. 1 Normalized absorption of the PDTBDT-DTBT and PDTBDT-DTFBT in dilute solution and thin film.

For the CP in dilute solution, the molecule motions of conjugated polymer was accelerated when the temperature elevated, which resulted in the absorption shoulder peaks related to aggregation produced by intermolecular π–π* transitions will be reduced at long wavelength range during heating process. Meanwhile, the distortion of the conjugated backbone was strengthened with the raising temperature, which led to the decreasing of effective conjugation length of polymer backbone, and thus absorption peaks originated from the localized π–π* transitions and ones produced by ICT transitions were both blue-shifted.[19a,27,28] Moreover, the conjugation length would be decreased because of more twisting or decreased coplanarity of the building blocks in the repeating units at a higher temperature, thus led to the blue-shift of the absorption peaks originated from to π–π* transition along the CP backbones.[14b,19] To verify the above conditions, temperature-dependent absorption (TD-Abs) spectra of the PDTBDT-DTBT, PDTBDT-DTFBT in CB solution were also measured. As shown in Fig. 2a and b, obvious changing of absorption spectra of PDTBDT-DTBT and PDTBDT-DTFBT in CB were found during the heating process, and the thermochromic effect from a blue solution to a red solution was observed. From 15 to 95 °C, the absorbance of the former 0–0 peaks at 680 nm for PDTBDT-DTBT decreased continuously, and then disappeared while the temperature was increased from 95 to 115 °C. As compared with PDTBDT-DTBT, the TD-Abs spectra of the PDTBDT-DTFBT, the absorbance of the former 0–0 peaks at 662 nm for PDTBDT-DTFBT presented similar temperature-dependent variation in relative to those for PDTBDT-DTBT during the heating process, except that the 0–0 peaks at 662 nm did not disappeared even the temperature was increased to 115 °C. As expected, the peaks at 630 nm for PDTBDT-DTBT and 612 nm for PDTBDT-DTFBT, which were originated from the ICT along the conjugated backbones of the PDTBDT-DTBT and PDTBDT-DTFBT, were continuously blue-shifted from 630 to 546 nm and 612 to 549 nm as the temperature were increased from 15 to 115 °C. As compared with the absorption characteristics of PDTBDT-DTBT and PDTBDT-DTFBT, the thermochromic effect from a blue solution to a red solution was observed in the solution of PDTBDT-BT and PDTBDT-FBT (see ESI, Fig. S3†). These results verified that the PDTBDT-DTBT and PDTBDT-DTFBT can establish strong interchain π–π* interaction even in dilute solution, and the insertion of alkylthiophene spacers would result in the increase of the polymer chains aggregation even in dilute solution. Meanwhile, the evidences that the increase of the temperature

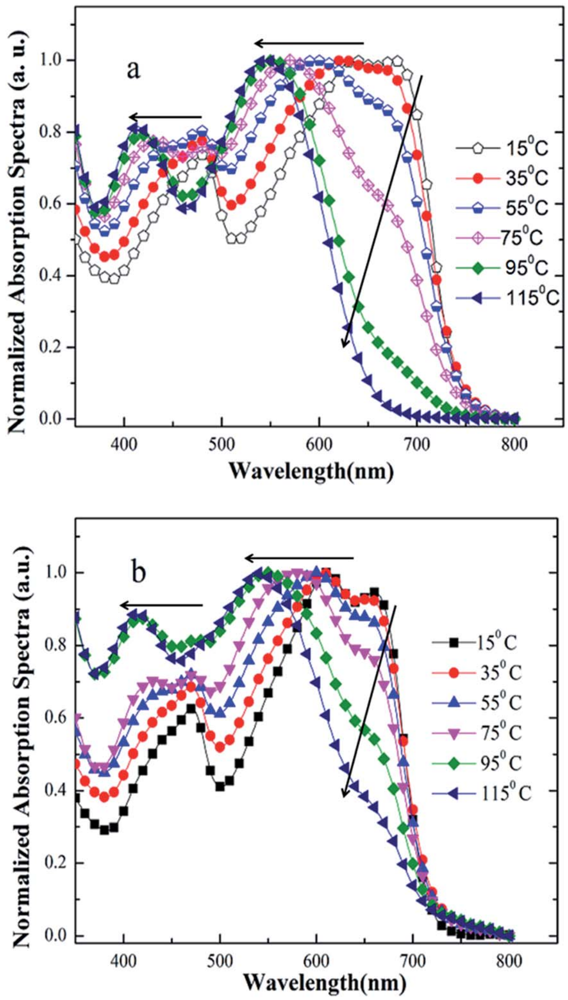

Fig. 2 Temperature-dependent UV-vis spectra of PDTBDT-DTBT (a) and PDTBDT-DTFBT (b) in chlorobenzene solution.

of the solutions resulted in the continuously blue-shifting of the main photoluminescence (PL) peaks and decrease shoulder PL peaks of the PDTBDT-DTBT and PDTBDT-DTFBT (see ESI, Fig. S3 and S5†), the enlarging of the alkyl side chains of the alkylthiophene spacers reduced the π–π* interaction and increased the twisting freedom of the conjugation backbone of the copolymers in dilute solution, thus result in the easier change of the absorption peaks of the interchain π–π* interaction and the π–π* transition along the CP backbones during the heating process (see ESI, Fig. S4 and S6†), were also supported the above deductions. In addition to the above features, we observed that not only the absorption peaks originated from ICT of PDTBDT-DTFBT at around 662 nm (Fig. 2a and b), but also the main PL peaks and shoulder PL emission at longer wavelength were less effected by increase of the temperature in relative to those for the PDTBDT-DTBT (see ESI, Fig. S3 and S5†). It might illustrate that the PDTBDT-DTFBT exhibited stronger interchain π–π* interaction than that for PDTBDT-DTBT in dilute solution, and the insertion of fluorine atom also played positive effect on the increase of the rigidity and interchain π–π* interaction of the copolymers.[19]

To understand the effect of the insertion of fluorine atoms on the interchain π–π* interaction and thermochromic properties of the copolymers, calculations were implemented by using density functional theory (DFT) calculation with B3LYP/6-31G(d,p) basis set in Gaussian 09 (ref. 20) under striking an balance between prediction of the conformation and a completion of the calculations within reasonable time, and the alkyl side substituents were replaced as methyl. The *trans*- (or *cis*-) coplanar conformations of the PDTBDT-DTBT and PDTBDT-DTFBT were respectively defined by the dihedral angles (torsion angels) between the alkylthiophene spacers (T) and benzothiadiazole (BT) or 5,6-difluorobenzothiadiazole (FBT) for −90° and 270° (Fig. 3a). The optimized ground-state geometries of the PDTBDT-DTBT and PDTBDT-DTFBT systems were demonstrated to be *trans*-conformation, in which the dihedral angle of between T and BT in PDTBDT-DTBT systems were 7.7°, while the angles between T and FBT became 0.3° in PDTBDT-DTFBT (Fig. 3b). The relaxed potential-energy scans and relative populations of the T-BT and T-FBT link bond signified that the T-FBT link exhibited narrower potential energy wells than that for the T-BT link, and the PDTBDT-DTFBT system exhibited a narrower distribution of conformations around the *trans*-coplanar conformer (0°) compared to that for PDTBDT-DTBT system (Fig. 3c and d). The above results indicate that the insertion of fluorine atoms would contribute to the significant enhancement of the planarity and rigidity of the PDTBDT-DTFBT, and the smaller rotating energy barrier near the minimum energy conformation of T-FBT link in contrast to that for T-BT link, all of which would led to the stronger interchain π–π* interaction and more difficult thermochromic of the PDTBDT-DTFBT as compared PDTBDT-DTBT during the heating process.

2.3. Electrochemical characteristics of the copolymers

To investigate the influence of the insertion of the alkylthiophene and fluorine atom on the energy levels of the polymers, the electrochemical behaviors of the copolymers of the PDTBDT-DTBT and PDTBDT-DTFBT were investigated by cyclic voltammetry (CV) in a nitrogen-saturated acetonitrile solution containing 0.1 M tetrabutylammonium hexafluoro-phosphate with glass carbon, $Ag/AgNO_3$ and Pt wire electrode as the working, reference and counter electrode, respectively. All scans were performed at a scan rate of 50 mV s^{-1}. The oxidation potential of PDTBDT-DTBT and PDTBDT-DTFBT were respectively observed at around, 0.48 V and 0.57 V. The redox potential of Fc/Fc^+ in the above-mentioned condition is +0.09 V, which is assumed to have an absolute energy level of −4.8 eV to vacuum for calibration. The HOMO and LUMO levels calculated by empirical formulas ($E_{HOMO} = -(E_{ox} + 4.71)$ (eV)[21] and $E_{LUMO} = -(|HOMO| - E_g)$ (eV)), were about −5.19 eV and −3.57 eV for PDTBDT-DTBT, −5.28 eV and −3.57 eV for PDTBDT-DTFBT, respectively. As compared with those for the copolymers without alkylthiophene spacers (PDTBDT-BT and PDTBDT-FBT) (see ESI, Fig. S7 and S8†), the HOMO and LUMO energy levels of copolymers with alkylthiophene spacers (PDTBDT-DTBT and PDTBDT-DTFBT) were clearly raised (Table 1 and Fig. 4). It indicated that the insertion of alkylthiophene spacers would lead to the increase of the HOMO energy levels and

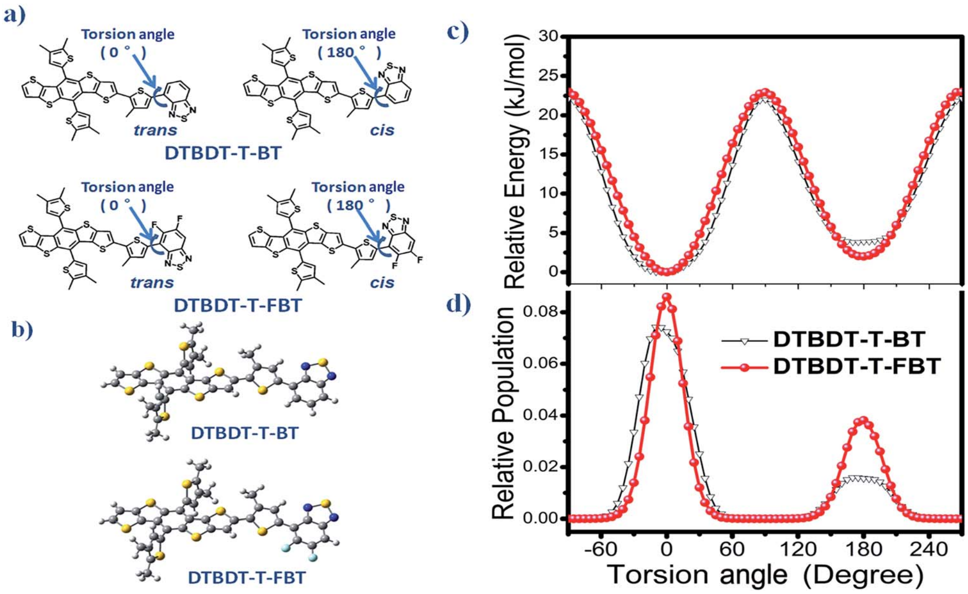

Fig. 3 (a) The *trans*-(or *cis*-) coplanar conformations of the PDTBDT-DTBT and PDTBDT-DTFBT defined by the dihedral (torsion angels between the alkylthiophene and BT (or FBT)); (b) the optimal geometries at the B3LYP/6-31G(d,p) level; (c) potential energy scan profiles of the DTBDT-T-BT and DTBDT-T-FBT as a functional of the torsion angels; (d) relative population of optimal conformations with a Boltzmann energy distribution at room temperature.

LUMO energy levels for copolymers derived from DTBDT-T and BT derivatives. Meanwhile, it also could be noticed that the insertion of fluorine atoms would result in the deepening of the HOMO and LUMO energy levels, but the effect on the deepening of the HOMO levels are much significant that those on the LUMO levels. The DFT calculations of the trimers of copolymers predicated approximate HOMO/LUMO energies of −4.67/−2.76 eV for PDTBDT-DTBT, −4.75/−2.81 eV for PDTBDT-DTFBT, −4.81/−2.83 eV for PDTBDT-BT and −4.94/−2.94 eV for PDTBDT-FBT (see ESI, Fig. S9–S12†), which are in general agreement with the experimental evidences that the insertion of alkylthiophene would result in the increase of the HOMO and LUMO, and insertion of fluorine atom would result in the decreases of HOMO and LUMO, but it provides little effect on the LUMO energy levels in relative to

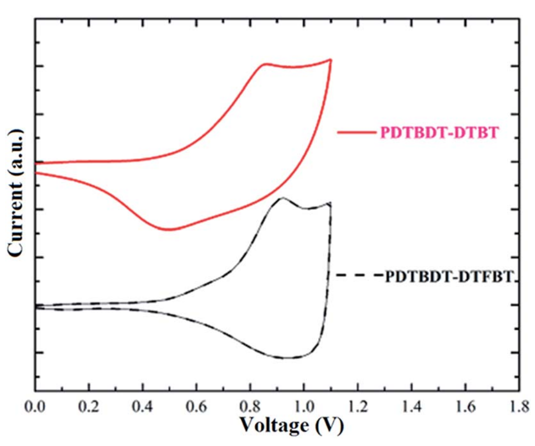

Fig. 4 Cyclic voltammetry curves of the PDTBDT-DTBT and PDTBDT-DTFBT.

the decrease of the HOMO energy levels, which were contributed to the inductively withdrawing and mesomerically donating properties of the fluorine atoms.[22]

2.4. 2D incident wide-angle X-ray scattering (GIWAXS) and SCLC analysis

Two-dimensional grazing incident wide-angle X-ray scattering (2D-GIWAXS) measurement (see ESI, Fig. S13 and S14†) was used to characterize the crystalline structural features of the polymers neat films.[23] PDTBDT-DTBT and PDTBDT-DTFBT samples present broad peaks (100) at ∼0.23 and ∼0.22 $Å^{-1}$, corresponding to a lamellar *d*-spacing of 26.8 and 28.5 Å, respectively. The reflection (010) peaks of the PTBDT-DTBT and PDTBDDTFBT could be observed at 1.69 $Å^{-1}$, which corresponds to the *d*-spacing for π–π stacking of 3.7 Å. As compared with the lamellar *d*-spacing of 21 Å and 3.8 Å of the *d*-spacing for π–π stacking for the copolymers of PDTBDT-BT and PDTBDT-FBT,[7b] the lamellar *d*-spacing of PDTBDT-DTBT and PDTBDT-DTFBT were increased, and the *d*-spacing for π–π stacking of the PDTBDT-DTBT and PDTBDT-DTFBT were slightly decreased. The increase of the lamellar *d*-spacing of the PDTBDT-DTBT and PDTBDT-DTFBT would be contribute to the increased of the sum of alkyl side chains, and the decrease of the *d*-spacing for π–π stacking of the PDTBDT-DTBT and PDTBDT-DTFBT would be contributed to the enhancement of the π–π stacking by insertion of the alkylthiophene spacers. More detailed analyses of the out-of-plane and in-plane of the PDTBDT-DTBT and PDTBDT-DTFBT revealed that the PDTBDT-DTFBT exhibited enhanced π–π stacking, which were consistent with those from the TD-UV absorption and computational calculations predicated that the insertion of fluorine would result in the increase of the interchain π–π* interaction and the planarity and rigidity of the PDTBDT-DTFBT. The mobility of PDTBDT-DTBT and PDTBDT-DTFBT, which were determined by applying the space-charge limited current (SCLC) model,[3] were found to be 1.28×10^{-4} and 2.17×10^{-4} $cm^2 V^{-1} s^{-1}$ (see ESI, Fig. S15†), respectively. Considering above results, it was concluded that the insertion of the alkylthiophene and fluorine atoms would result in the enhancement of the enhanced π–π stacking and hole mobility of the copolymers derived from DTBDT and copolymers derived from DTBDT and BT derivatives.

2.5. Photovoltaic properties of the copolymers

The copolymers of PDTBDT-DTBT and PDTBDT-DTFBT, as the electron donor materials for PVCs, were employed in PVCs with device configuration of ITO/PEDOT:PSS/active layer/Ca/Al, and $PC_{71}BM$ as the electron acceptor materials. The weight ratios of the copolymers and $PC_{71}BM$ were varied from 1 : 1 to 1 : 2 and then up to 1 : 3 with 3% 1,8-diiodooctane (DIO) as solvent additives. And the devices were characterized under AM 1.5 simulator (100 mW cm^{-2}). The PCEs of the PVCs from PDTBDT-DTBT/$PC_{71}BM$ were varied from 4.77% to 6.04% and then dropped to 4.61% with the open circuit voltage (V_{oc}) of 0.63–0.65 V, short current densities (J_{sc}) ranging from 12.21–15.64 mA cm^{-2} and fill factor (FF) ranging from 55.36–61.95% (Fig. 5a, Table 2), while the weight ratios of PDTBDT-DTBT and $PC_{71}BM$ were varied from 1 : 1 to 1 : 2 and then up to 1 : 3. It could be found that the optimal weight ratio of PDTBDT-DTBT and $PC_{71}BM$ was 1 : 2. Meanwhile, the maximal PCE of 7.12% was achieved in the PVCs from PDTBDT-DTFBT/$PC_{71}BM$ with the V_{oc} of 0.73 V, J_{sc} of 15.10 mA cm^{-2} and FF of 64.55%, and the PCEs of the devices from PDTBDT-DTFBT and $PC_{71}BM$ were also increased at beginning and then dropped while the weight ratios of PDTBDT-DTFBT and $PC_{71}BM$ were varied from 1 : 1 to 1 : 2 and then to 1 : 3 (Fig. 5b). The comparative AFM investigations of the optimal weight ratio blend films from PDTBDT-DTBT/$PC_{71}BM$ and PDTBDT-DTFBT/$PC_{71}BM$ with and/or without DIO as solvent additives confirmed that the induction of DIO would result in the amelioration of the morphologies the blend films (see ESI, Fig. S16 and S17†), which would contribute to the improvement of the J_{sc} and FF of the corresponding devices (Fig. 5a and b and Table 2). The deviations between the integral current density and the J_{sc} read from the *J*–*V* measurements of the PVCs with the optimal weight ratios of the copolymers and $PC_{71}BM$ are within 3%, indicating the consistency of photovoltaic results (Fig. 5c).

2.6. Dielectric constant of the copolymers

Besides lowering the HOMO energy levels, aggregation and charge transporting properties *etc.* of CPs,[24] it has been suggested that the insertion of the fluorine substituents would contribute to the increase of the dielectric constants, thus result in the suppression of the bimolecular (non-geminate) recombination rates.[25] Mitigation of the space charge effects, and possibly decrease of the effect of the insertion of fluorine substituents on the relative dielectric constants (ε_r) of the copolymers, the refractive indices

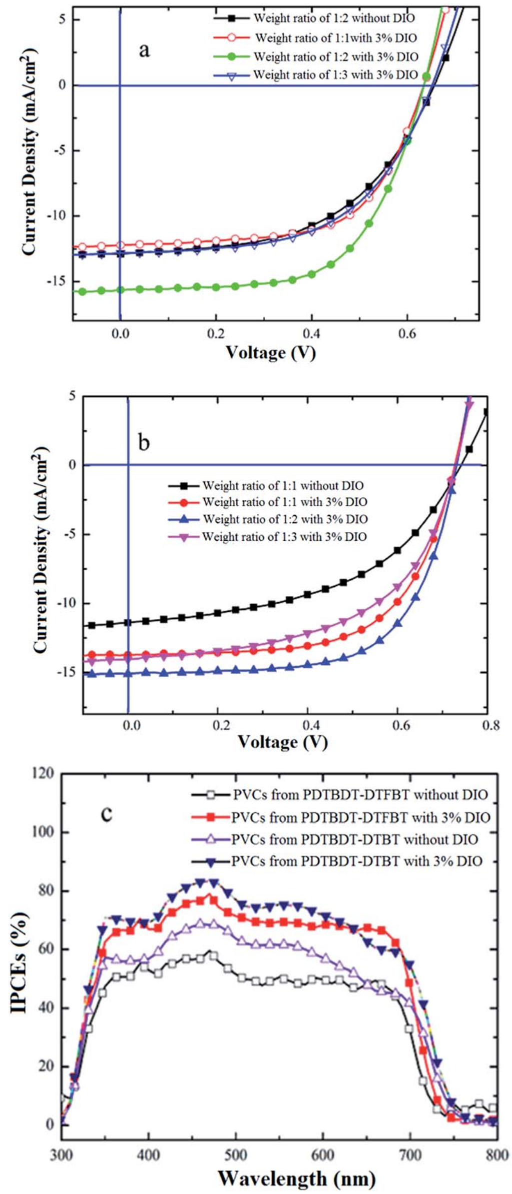

Fig. 5 *J*–*V* characteristics for the PVCs based on PDTBDT-DTBT: $PC_{71}BM$ (a) and PDTBDT-DTFBT: $PC_{71}BM$ (b) and the corresponding IPCEs curves (c).

(*n*) and extinction co-efficiencies (*k*) of the copolymer were determined by ellipsometers as the dielectric constants could be determined by the equations:[26]

$$\varepsilon_r = n^2 - k^2 \quad (1)$$

As shown in Fig. 6a and b, the refractive indices of the PDTBDT-DTBT and PDTBDT-DTFBT were trended to constant values of 1.70 and 1.69 while the extinction co-efficiencies of them were trended to be negligible at 1700 nm. The relative dielectric constants of PDTBDT-DTBT and PDTBDT-DTFBT were about 2.86 and 2.85 for PDTBDT-DTBT and PDTBDT-DTFBT at 1700 nm, respectively. These results verified that

Table 2 Parameters of the optimal of the photovoltaic cells from PDTBDT-DTBDT/$PC_{71}BM$ and PDTBDT-DTFBT/$PC_{71}BM$

Active layers	DIO (%)	V_{oc} (V)	J_{sc} (mA cm^{-2})	FF (%)	η (%)
PDTBDT-DTBT/$PC_{71}BM$ (w/w; 1 : 1.5)	0%	0.66	12.89 (12.63)[a]	51.74	4.40
	3%	0.63	15.64 (15.75)[a]	61.28	6.04
PDTBDT-DTFBT/$PC_{71}BM$ (w/w; 1 : 1.5)	0%	0.74	11.39 (11.13)[a]	48.75	4.11
	3%	0.73	15.10 (14.88)[a]	64.55	7.12

[a] The integral current density calculated from IPCE data.

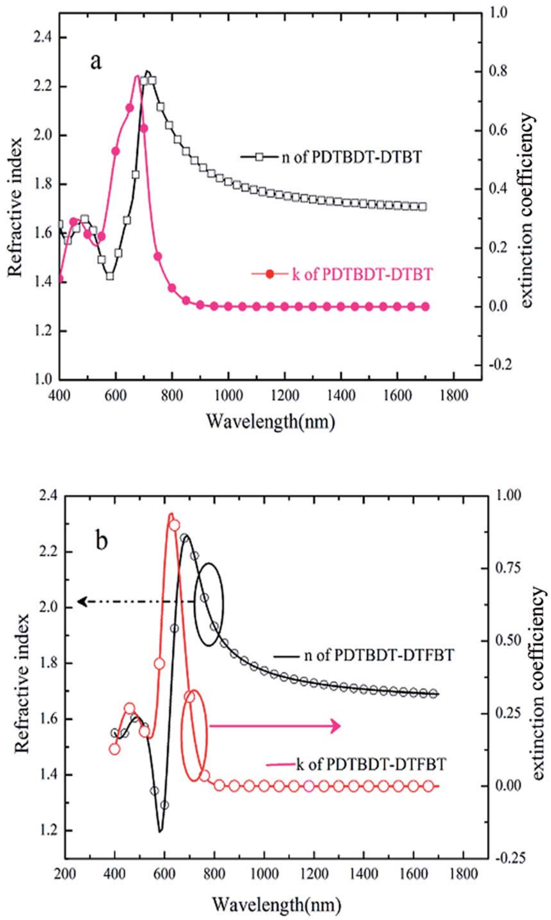

Fig. 6 Extinction co-efficiencies and refractive index of PDTBDT-DTBT (a) and PDTBDT-DTFBT (b) determined by ellipsometers.

the insertion of the fluorine substituents did not result in the increase of the relative dielectric constants of the copolymers derived from DTBT and/or DTFBT with alkylthiophene spacers. It was noticed that the consistency between the measured V_{oc} and calculated V_{oc} of the PVCs from PDTBDT-DTBT/$PC_{71}BM$ and/or PDTBDT-DTFBT/$PC_{71}BM$ blend films by suggested empirical equation under consideration of the difference of the HOMO energy levels of the copolymers and LUMO energy levels of $PC_{71}BM$ (see ESI, Fig. S18†), were also supported that the insertion of the fluorine substituents did not result in the increase of the dielectric constants of the PDTBDT-DTFBT.[25]

3. Conclusion

Alternating conjugated polymers based on 5,10-bis(dialkylthien-2-yl)dithieno[2,3-*d*:2′,3′-*d*′]benzo[1,2-*b*:4,5-*b*′]dithiophene (DTBDT) and benzothiadiazole and/or 5,6-difluorobenzothiadiazole with alkylthiopene spacers were synthesized, and the effect of insertion of alkylthiophene spacers and fluorine atoms on the characteristics of the copolymers, such as, the energy levels, intrachain π–π interaction, dielectric constants and photovoltaic properties *etc.*, were systematically investigated. The insertion of alkylthiophene spacers not only led to the increase of the intrachain interaction of the copolymers, which resulted in the copolymers with alkylthiophene spacers exhibited strong intrachain π–π interaction, but also led to the increase of HOMO and LUMO energy levels. The insertion of the fluorine atoms resulted in the decrease of both HOMO and LUMO energy levels with the enhancement of the planarity and hole mobility. However, the inclusion of fluorine atoms provided little effect on the LUMO levels in relative to the decrease of the HOMO levels, and almost did not affect the dielectric constant of the copolymer. Use of the materials in polymeric photovoltaic cells lead to high performance PVCs with PCEs of 6.04–7.12%. These results demonstrated that the opto-electronic and aggregation properties of the 5,10-bis(dialkylthien-2-yl)dithieno[2,3-*d*:2′,3′-*d*′]benzo[1,2-*b*:4,5-*b*′]dithiophene-*alt*-benzothiadiazole derivatives copolymers can be effectively regulated by the introduction of alkylthiophene spacers and/or fluorine atoms into the backbone.

4. Experimental section

4.1. Materials

All reagents, unless otherwise specified, were obtained from Aldrich, Acros and TCI Chemical Co., and used as received. The THF were dried by sodium with benzophenone as indicator under a nitrogen flow. 2,7-Di(trimethylstannyl)-5,10-bis(4,5-didecylthien-2-yl)dithieno[2,3-*d*:2′,3′-*d*′]benzo[1,2-*b*:4,5-*b*′]dithiophene (DTBDT-TSn),[3a] 4,7-bis(5-bromo-4-octylthien-2-yl)-2,1,3-benzothiadiazole ($DTBTBr_2$)[13] and 4,7-bis(5-bromo-4-octylthien-2-yl)-5,6-difluoro-2,1,3-benzothiadiazole ($DTFBTBr_2$),[14] 4,7-bis(5-bromo-4-dodecylthien-2-yl)-2,1,3-benzothiadiazole ($DTBTC12Br_2$)[3a] and 4,7-bis(5-bromo-4-dodecylthien-2-yl)-5,6-difluoro-2,1,3-benzothiadiazole ($DTFBTC12Br_2$)[14] were synthesized as the procedure reported in the reference, and characterized by ^{1}H NMR before use.

4.2. General method

^{1}H NMR spectra were recorded on a Bruker DRX 400 spectrometer operating at 400 MHz and were referred to tetramethylsilane. Analytical GPC was performed using a Waters GPC 2410 in tetrahydrofuran (THF) relative to polystyrene standards. Thermal gravimetric analysis (TGA) was conducted on a TGA 2050 (TA instruments) thermal analyses system under a heating rate of 10 °C min^{-1} and a nitrogen flow rate of 20 mL min^{-1}. UV-vis absorption spectra were measured on a UV-2500 spectrophotometer (Shimadzu. Co.). The cyclic voltammetry (CV) was measured on CHI 660 electrochemical workstation (Shanghai Chenhua Co.) at a scan rate of 50 mV s^{-1} with a nitrogen-saturated solution of 0.1 M tetrabutylammonium hexafluorophosphate (Bu_4NPF_6) in acetonitrile (CH_3CN) with glass carbon and Ag/$AgNO_3$ electrode as the working and reference electrode, respectively. Tapping-mode atomic force microscopy (AFM) images were obtained using a NanoScope NS3A system (Digital Instrument). The refractive indices and extinction coefficients of each layer were measured on Horiba Jobin Yvon AUTO SE ellipsometer. The 2D grazing-incidence wide-angle X-ray scattering (GIWAXS) measurements were performed at the Stanford Synchrotron Radiation Lightsource (SSRL) on Beamline 11-3, with a MAR345 image plate area detector, at 12.7 keV incident photon energy.

4.3. Preparation and characterization of the photovoltaic solar cells

A patterned indium tin oxide (ITO) coated glass with a sheet resistance of 10–15 Ω per square was cleaned by a surfactant scrub, followed by a wet-cleaning process inside an ultrasonic bath, beginning with de-ionized water, followed by acetone and isopropanol. After oxygen plasma cleaning for 5 min. The regular devices with thermally-evaporated Ca (8 nm) and Al (100 nm) as cathode and an ITO substrate coated with a PEDOT:PSS interfacial layer as the anode, were prepared as the follow processes: a 40 nm thick poly(3,4-ethylenedioxythiophene):poly(styrene sulfonate) (PEDOT:PSS) (Bayer Baytron 4083) anode buffer layer was spin-casted onto the ITO substrate and then dried by baking in a vacuum oven at 80 °C overnight. The active layers, with a thickness in the 80–90 nm range, were then deposited on top of the PEDOT:PSS layer by spin-casting from the *o*-dichlorobenzene solution containing copolymers of PDTBDT-DTBT and/or PDTBDT-DTFBT and $PC_{71}BM$ with weight ratios of 1 : 1, 1 : 2 and 1 : 3. Then a 8 nm Ca and 100 nm Al evaporated with a shadow mask under vacuum of (1–2) × 10^{-4} Pa. The overlapping area between the cathode and anode defined a pixel size of device of 0.1 cm^2. The thickness of the evaporated cathode was monitored by a quartz crystal thickness/ratio monitor (SI-TM206, Shenyang Sciences Co.). Except for the deposition of the PEDOT:PSS layers, all the fabrication processes were carried out inside a controlled atmosphere in a nitrogen drybox (Etelux Co.) containing less than 1 ppm oxygen and moisture. The PCEs of the resulting polymer solar cells were measured under 1 sun, AM 1.5G (air mass 1.5 global) condition using a solar simulator (XES-70S1, San-EI Electric Co.) with irradiation of 100 mW cm^{-2}. The current density–voltage (*J*–*V*) characteristics were recorded with a Keithley 2400 source-measurement unit. The spectral responses of the devices were measured with a commercial EQE/incident photon to charge carrier efficiency (IPCE) setup (7-SCSpecIII, Beijing 7-star Opt. In. Co.). A calibrated silicon detector was used to determine the absolute photosensitivity.

4.4. Synthesis copolymers

4.4.1. Synthesis of PDTBDT-DTBT. A mixture of toluene (6 mL) and *N*,*N*-dimethylformamide (DMF, 0.7 mL) were added to a 55 mL microwave tube containing DTBDT-Sn (270.7 mg, 0.2 mmol), 4,7-bis(5-bromo-4-octylthien-2-yl)-2,1,3-benzothiadiazole ($DTBTBr_2$) (136.5 mg, 0.2 mmol) and $Pd(PPh_3)_4$ (4.0 mg) in a glove box with moisture and oxygen under 1 ppm. Then the tube was subjected to the following reaction conditions in a microwave reactor: 120 °C for 5 min, 140 °C for 5 min and 160 °C for 20 min. At the end of polymerization, the polymer was end-capped with 2-(tributylstannyl)thiophene and 2-bromothiophene to remove bromo and trimethystannyl end groups. The mixture was then poured into methanol. The precipitated material was collected and extracted with ethanol, acetone, hexane and toluene in a Soxhlet extractor. The solution of the copolymer in toluene was condensed to 20 mL and then poured into methanol (500 mL). The precipitation was collected and dried under vacuum overnight (yield: 75%). M_n = 26 130 g mol^{-1} with a polydisperse index (PDI) of 2.46.

4.4.2. Synthesis of PDTBDT-DTFBT. The PDTBDT-DTFBT was synthesized as the procedure of PDTBDT-DTBT, except that the polymerization was carried out with DTBDT-TSn (270.7 mg, 0.2 mmol), $DTFBTBr_2$ of (143.7 mg, 0.2 mmol). Yield: 80%. M_n = 37 440 g mol^{-1} with PDI of 3.17.

4.4.3. Synthesis of PDTBDT-DTBTC12. The PDTBDT-DTFBT was synthesized as the procedure of PDTBDT-DTBT, except that the polymerization was carried out with DTBDT-TSn (270.7 mg, 0.2 mmol), $DTBTC12Br_2$ (159.0 mg, 0.2 mmol). Yield: 83%. M_n = 41 060 g mol^{-1} with PDI of 3.22.

4.4.4. Synthesis of PDTBDT-DTFBTC12. The PDTBDT-DTFBT was synthesized as the procedure of PDTBDT-DTBT, except that the polymerization was carried out with DTBDT-TSn (270.7 mg, 0.2 mmol), $DTFBTC12Br_2$ (166.2 mg, 0.2 mmol). Yield: 78%. M_n = 34 640 g mol^{-1} with PDI of 2.88.

Acknowledgements

The authors are deeply grateful to National Nature Science Foundation of China (51463011, 91333206, 61264002, 61404067, 51602139), open fund of State Key Laboratory of Infrared Physics (Z201302), the Program for New Century Excellent Talents in University of Ministry of Education of China (Grant No. NCET-13-0840), and China Scholarship Council for financial support.

Notes and references

1 (*a*) P. Gao, D. Beckmann, H. N. Tsao, X. Feng, V. Enkelmann, M. Baumgarten, W. Pisula and K. Müllen, *Adv. Mater.*, 2009, **21**, 213; (*b*) Y. Wu, Z. Li, X. Guo, H. Fan, L. Huo and J. Hou, *J.*

Mater. Chem., 2012, **22**, 21362; (*c*) Y. Wu, Z. Li, W. Ma, Y. Huang, L. Huo, X. Guo, M. Zhang, H. Ade and J. Hou, *Adv. Mater.*, 2013, **25**, 3449; (*d*) H.-J. Yun, Y.-J. Lee, S.-J. Yoo, D. S. Chung, Y.-H. Kim and S.-K. Kwon, *Chem.–Eur. J.*, 2013, **19**, 13242.

2 (*a*) H. J. Son, L. Lu, W. Chen, T. Xu, T. Zheng, B. Carsten, J. Strzalka, S. B. Darling, L. X. Chen and L. Yu, *Adv. Mater.*, 2012, **25**, 838; (*b*) N. Shin, H.-J. Yun, Y. Yoon, H. J. Son, S.-Y. Ju, S.-K. Kwon, B. S. Kim and Y.-H. Kim, *Macromolecules*, 2015, **48**, 3890.

3 (*a*) S. Sun, P. Zhang, J. Li, Y. Li, J. Wang, S. Zhang, Y. Xia, X. Meng, D. Fan and J. Chu, *J. Mater. Chem. A*, 2014, **2**, 15316; (*b*) T. I. Ryu, Y. Yoon, J.-H. Kim, D.-H. Hwang, M. J. Ko, D.-K. Lee, J. Y. Kim, H. Kim, N.-G. Park, B. S. Kim and H. J. Son, *Macromolecules*, 2014, **47**, 6270; (*c*) S. Park, B. T. Lim, B. S. Kim, H. J. Son and D. S. Chung, *Sci. Rep.*, 2016, **4**, 5482.

4 C. Lang, J. Fan, Y. Gao, M. Liu, Y. Zhang, F. Guo and L. Zhao, *Dyes Pigm.*, 2017, **137**, 50.

5 Y. J. Kim, M.-J. Kim, T. K. An, Y.-H. Kim and C. E. Park, *Chem. Commun.*, 2015, **51**, 11572.

6 P. Guo, Y. Xia, F. Huang, G. Luo, J. Li, P. Zhang, Y. Zhu, C. Yang, H. Wu and Y. Cao, *RSC Adv.*, 2015, **5**, 12879.

7 (*a*) W. Zhong, J. Xiao, S. Sun, X.-F. Jiang, L. Lan, L. Ying, W. Yang, H.-L. Yip, F. Huang and Y. Cao, *J. Mater. Chem. C*, 2016, **4**, 4719; (*b*) H. S. Lee, H. G. Song, H. Jung, M. H. Kim, C. Cho, J.-Y. Lee, S. Park, H. J. Son, H.-J. Yun, S.-K. Kwon, Y.-H. Kim and B. S. Kim, *Macromolecules*, 2016, **49**, 7844.

8 Y. Xia, H. Zhang, J. Li, J. Tong, P. Zhang and C. Yang, *J. Polym. Res.*, 2015, **22**, 633.

9 L. Huo, T. Liu, X. Sun, Y. Cai, A. J. Heeger and Y. Sun, *Adv. Mater.*, 2015, **27**, 2938.

10 (*a*) M. C. Scharber, D. Mühlbacher, M. Koppe, P. Denk, C. Waldauf, A. J. Heeger and C. J. Brabec, *Adv. Mater.*, 2006, **18**, 789; (*b*) Y. Li, *Acc. Chem. Res.*, 2012, **45**, 723; (*c*) H. Zhou, L. Yang and W. You, *Macromolecules*, 2012, **45**, 607; (*d*) Z.-G. Zhang and J. Wang, *J. Mater. Chem.*, 2012, **22**, 4178; (*e*) L. Lu, T. Zheng, Q. Wu, A. M. Schneider, D. Zhao and L. Yu, *Chem. Rev.*, 2015, **115**, 12666.

11 (*a*) L. Biniek, S. Fall, C. L. Chochos, D. V. Anokhin, D. A. Ivanov, N. Leclerc, P. Lévêque and T. Heiser, *Macromolecules*, 2010, **43**, 9779; (*b*) X. Wang, Y. Sun, S. Chen, X. Guo, M. Zhang, X. Li, Y. Li and H. Wang, *Macromolecules*, 2012, **45**, 1208; (*c*) Y. Wang, X. Xin, Y. Lu, T. Xiao, X. Xu, N. Zhao, X. Hu, B. S. Ong and S. C. Ng, *Macromolecules*, 2013, **46**, 9587; (*d*) I. Osaka, T. Kakara, N. Takemura, T. Koganezawa and K. Takimiya, *J. Am. Chem. Soc.*, 2013, **135**, 8834; (*e*) Y. Liu, J. Zhao, Z. Li, C. Mu, W. Ma, H. Hu, K. Jiang, H. Lin, H. Ade and H. Yan, *Nat. Commun.*, 2014, **5**, 5293; (*f*) S. Liu, X. Bao, W. Li, K. Wu, G. Xie, R. Yang and C. Yang, *Macromolecules*, 2015, **48**, 2948; (*g*) N. Zhou, X. Guo, R. P. Ortiz, T. Harschneck, E. F. Manley, S. J. Lou, P. E. Hartnett, X. Yu, N. E. Horwitz, P. M. Burrezo, T. J. Aldrich, J. T. L. Navarrete, M. R. Wasielewski, L. X. Chen, R. P. H. Chang, A. Facchetti and T. J. Marks, *J. Am. Chem. Soc.*, 2015, **137**, 12565; (*h*) H. Zheng, J. Wang, W. Chen, C. Gu, J. Ren, M. Qiu, R. Yang and M. Sun, *J. Mater. Chem. C*, 2016, **4**, 6280; (*i*) J. Lee, M. Kim, B. Kang, S. B. Jo, H. G. Kim, J. Shin and K. Cho, *Adv. Energy Mater.*, 2014, **4**, 1400087.

12 (*a*) Z. Ma, D. Dang, Z. Tang, D. Gedefaw, J. Bergqvist, W. Zhu, W. Mammo, M. R. Andersson, O. Inganäs, F. Zhang and E. Wang, *Adv. Energy Mater.*, 2013, **4**, 1301455; (*b*) S.-C. Lan, P.-A. Yang, M.-J. Zhu, C.-M. Yu, J.-M. Jiang and K.-H. Wei, *Polym. Chem.*, 2013, **4**, 1132.

13 Y. Xia, X. Deng, L. Wang, X. Li, X. Zhu and Y. Cao, *Macromol. Rapid Commun.*, 2006, **27**, 1260.

14 (*a*) L. Dou, C.-C. Chen, K. Yoshimura, K. Ohya, W.-H. Chang, J. Gao, Y. Liu, E. Richard and Y. Yang, *Macromolecules*, 2013, **46**, 3384; (*b*) Z. Chen, P. Cai, J. Chen, X. Liu, L. Zhang, L. Lan, J. Peng, Y. Ma and Y. Cao, *Adv. Mater.*, 2014, **26**, 2586.

15 B. Carsten, F. He, H. J. Son, T. Xu and L. Yu, *Chem. Rev.*, 2011, **111**, 1493.

16 N. Blouin, A. Michaud and M. Leclerc, *Adv. Mater.*, 2007, **19**, 2295.

17 (*a*) C. Wang, X. Xu, W. Zhang, J. Bergqvist, Y. Xia, X. Meng, K. Bini, W. Ma, A. Yartsev, K. Vandewal, M. R. Andersson, O. Inganäs, M. Fahlman and E. Wang, *Adv. Energy Mater.*, 2016, **6**, 1600148; (*b*) Y. Li, X. Liu, F.-P. Wu, Y. Zhou, Z.-Q. Jiang, B. Song, Y. Xia, Z.-G. Zhang, F. Gao, O. Inganas, Y. Li and L.-S. Liao, *J. Mater. Chem. A*, 2016, **4**, 5890; (*c*) T. L. Nguyen, H. Choi, S.-J. Ko, M. A. Uddin, B. Walker, S. Yum, J.-E. Jeong, M. H. Yun, T. J. Shin, S. Hwang, J. Y. Kim and H. Y. Woo, *Energy Environ. Sci.*, 2014, **7**, 3040.

18 (*a*) N. Wang, W. Chen, W. Shen, L. Duan, M. Qiu, J. Wang, C. Yang, Z. Dua and R. Yang, *J. Mater. Chem. A*, 2016, **4**, 10212; (*b*) Z. Li, H. Lin, K. Jiang, J. Carpenter, Y. Li, Y. Liu, H. Hu, J. Zhao, W. Ma, H. Ade and H. Yan, *Nano Energy*, 2015, **15**, 607; (*c*) Y. Li, S.-J. Ko, S. Y. Park, H. Choi, T. L. Nguyen, M. A. Uddin, T. Kim, S. Hwang, J. Y. Kim and H. Y. Woo, *J. Mater. Chem. A*, 2016, **4**, 9967.

19 (*a*) H. Hu, K. Jiang, J.-H. Kim, G. Yang, Z. Li, T. Ma, G. Lu, Y. Qu, H. Ade and H. Yan, *J. Mater. Chem. A*, 2016, **4**, 5039; (*b*) S. Zhang, Y. Qin, M. A. Uddin, B. Jang, W. Zhao, D. Liu, H. Y. Woo and J. Hou, *Macromolecules*, 2016, **49**, 2993; (*c*) S. Zhang, B. Yang, D. Liu, H. Zhang, W. Zhao, Q. Wang, C. He and J. Hou, *Macromolecules*, 2016, **49**, 120.

20 M. J. Frisch, G. W. Trucks, H. B. Schlegel, G. E. Scuseria, M. A. Robb, J. R. Cheeseman, G. Scalmani, V. Barone, B. Mennucci, G. A. Petersson, H. Nakatsuji, M. Caricato, X. Li, H. P. Hratchian, A. F. Izmaylov, J. Bloino, G. Zheng, J. L. Sonnenberg, M. Hada, M. Ehara, K. Toyota, R. Fukuda, J. Hasegawa, M. Ishida, T. Nakajima, Y. Honda, O. Kitao, H. Nakai, T. Vreven, J. A. Montgomery Jr, J. E. Peralta, F. Ogliaro, M. Bearpark, J. J. Heyd, E. Brothers, K. N. Kudin, V. N. Staroverov, R. Kobayashi, J. Normand, K. Raghavachari, A. Rendell, J. C. Burant, S. S. Iyengar, J. Tomasi, M. Cossi, N. Rega, J. M. Millam, M. Klene, J. E. Knox, J. B. Cross, V. Bakken, C. Adamo, J. Jaramillo, R. Gomperts, R. E. Stratmann, O. Yazyev, A. J. Austin, R. Cammi, C. Pomelli, J. W. Ochterski, R. L. Martin, K. Morokuma, V. G. Zakrzewski, G. A. Voth,

P. Salvador, J. J. Dannenberg, S. Dapprich, A. D. Daniels, Ö. Farkas, J. B. Foresman, J. V. Ortiz, J. Cioslowski, and D. J. Fox, *Gaussian 09, revision A.01*, Gaussian, Inc., Wallingford CT, 2009.

21 J. Pommerehne, H. Vestweber, W. Guss, R. F. Mark, H. Bässles, M. Porsch and J. Daub, *Adv. Mater.*, 1995, **7**, 551.

22 (*a*) J. Wolf, F. Cruciani, A. El Labban and P. M. Beaujuge, *Chem. Mater.*, 2015, **27**, 4184; (*b*) Z. Wang, Z. Li, J. Liu, J. Mei, K. Li, Y. Li and Q. Peng, *ACS Appl. Mater. Interfaces*, 2016, **8**, 11639; (*c*) J. W. Jo, S. Bae, F. Liu, T. P. Russell and W. H. Jo, *Adv. Funct. Mater.*, 2015, **25**, 120; (*d*) J. W. Jo, J. W. Jung, E. H. Jung, H. Ahn, T. J. Shin and W. H. Jo, *Energy Environ. Sci.*, 2015, **8**, 2427; (*e*) M. Zhang, Xi. Guo, S. Zhang and J. Hou, *Adv. Mater.*, 2014, **26**, 1118.

23 J. Rivnay, S. C. B. Mannsfeld, C. E. Miller, A. Salleo and M. F. Toney, *Chem. Rev.*, 2012, **112**, 5488.

24 (*a*) A. C. Stuart, J. R. Tumbleston, H. Zhou, W. Li, S. Liu, H. Ade and W. You, *J. Am. Chem. Soc.*, 2013, **135**, 1806; (*b*) L. Yang, J. R. Tumbleston, H. Zhou, H. Ade and W. You, *Energy Environ. Sci.*, 2013, **6**, 316; (*c*) S. Albrecht, S. Janietz, W. Schindler, J. Frisch, J. Kurpiers, J. Kniepert, S. Inal, P. Pingel, K. Fostiropoulos, N. Koch and D. Neher, *J. Am. Chem. Soc.*, 2012, **134**, 14932.

25 (*a*) P. Yang, M. Yuan, D. F. Zeigler, S. E. Watkins, J. A. Lee and C. K. Luscombe, *J. Mater. Chem. C*, 2014, **2**, 3278; (*b*) N. Cho, C. W. Schlenker, K. M. Knesting, P. Koelsch, H.-L. Yip, D. S. Ginger and A. K.-Y. Jen, *Adv. Energy Mater.*, 2014, **4**, 1301857; (*c*) S. Chen, S.-W. Tsang, T.-H. Lai, J. R. Reynolds and F. So, *Adv. Mater.*, 2014, **26**, 6125; (*d*) Y. Lu, Z. Xiao, Y. Yuan, H. Wu, Z. An, Y. Hou, C. Gao and J. Huang, *J. Mater. Chem. C*, 2013, **1**, 630; (*e*) S. Chen, S. Tsang, T. Lai, J. R. Reynolds and F. So, *Adv. Mater.*, 2014, **26**, 6125.

26 (*a*) W. Frederick, *Optical Properties of Solids*, Academic Press, New York City, 1972, p. 49; (*b*) F. Hiroyukiara, *Spectroscopic Ellipsometry: Principles and Applications*, Wiley-VCH, Weinheim, 2007; (*c*) C. H. Ting and T. E. Seidel, *Mater. Res. Soc. Symp. Proc.*, 1995, **3**, 381; (*d*) S. M. Han and E. S. Aydil, *J. Appl. Phys.*, 1998, **83**, 2172.

27 C.-Y. Kuo, W. Nie, H. Tsai, H.-J. Yen, A. D. Mohite, G. Gupta, A. M. Dattelbaum, D. J. William, K. C. Cha, Y. Yang, L. Wang and H.-L. Wang, *Macromolecules*, 2014, **47**, 1008.

28 Q. Chu and Y. Pang, *Macromolecules*, 2003, **36**, 4614.